Semiclassical Theory of Vibrational Energy Relaxation in the Condensed Phase

Qiang Shi and Eitan Geva*

Department of Chemistry, University of Michigan, Ann Arbor, Michigan 48109-1055

Received: April 24, 2003; In Final Form: August 6, 2003

This paper presents the first application of semiclassical methodology to the calculation of vibrational energy relaxation (VER) rate constants in condensed phase systems. The VER rate constant is treated within the framework of the Landau−Teller formula and is given in terms of the Fourier transform, at the vibrational frequency, of the force−force correlation function (FFCF). Due to the high frequency of most molecular vibrations, predictions based on the *classical* FFCF are often found to deviate by orders of magnitude from the experimentally observed values. In this paper, we employ a semiclassical approximation for the quantum-mechanical FFCF, that puts it in terms of a classical-like expression, where Wigner transforms replace the corresponding classical quantities. The multidimensional Wigner transform is performed via a novel implementation of the local harmonic approximation (LHA). The resulting expression for the FFCF is exact at $t = 0$, and converges to the correct classical limit when $\hbar \rightarrow 0$. Quantum effects are introduced via a nonclassical initial sampling of both positions and momenta, as well as by accounting for delocalization in the calculation of the force at $t = 0$. The application of the semiclassical method is reported for three model systems: (1) a vibrational mode coupled to a harmonic bath, with the coupling exponential in the bath coordinates; (2) a diatomic coupled to a short linear chain of helium atoms; (3) a "breathing sphere" diatomic in a two-dimensional monatomic Lennard-Jones liquid. Good agreement is found in all cases between the semiclassical predictions and the exact results, or their estimates. It is also found that the VER of high-frequency molecular vibrations is dominated by a purely quantum-mechanical term, which vanishes in the classical limit.

I. Introduction

One of the most fundamental ways in which the environment affects solution-phase molecular dynamics (MD) is via vibrational relaxation. A typical situation involves energy relaxation of an excited vibrational mode, in a solute molecule, by energy transfer to other intermolecular and/or intramolecular accepting modes.[1−10] The rate of vibrational energy relaxation (VER) provides a sensitive probe of intramolecular dynamics and solute−solvent interactions, which are known to have a crucial impact on other important properties, such as chemical reactivity, solvation dynamics, and transport coefficients.

VER rates have been measured by time-domain pulsed laser techniques in a variety of hosts, including crystals, liquids, supercritical fluids, glasses, and proteins.[9−39] The observed VER lifetimes cover a wide range of time scales, extending from subpicoseconds to minutes, and reflect a rich variety of intermolecular and/or intramolecular pathways.

Most recent theoretical studies of VER have been based on either one of the following approaches: (1) *the direct approach*, which is based on nonequilibrium MD simulations; (2) *the perturbative approach*, which is based on extracting the force−force correlation function from equilibrium MD simulations.

The direct approach essentially mimics the experimental measurement of VER. It is based on performing nonequilibrium classical MD simulations, starting with an excited vibrational mode, and following its relaxation to equilibrium.[40−44] This approach is particularly useful in the case of low-frequency vibrational modes and/or high temperatures ($\hbar\omega/k_BT \ll 1$), for the following reasons: (1) A classical description of the relaxing vibrational mode and the relevant accepting modes is permissible when $\hbar\omega/k_BT \ll 1$. (2) In these cases, VER is fast due to the high density of accepting modes with matching frequencies, and can therefore be directly observed on the time scale accessible to classical MD simulations.

Unfortunately, low-frequency vibrations are the exception rather than the rule, and most molecular vibrations are characterized by high frequencies, such that $\hbar\omega/k_BT \gg 1$ even at room temperature. This situation has two important implications:

- VER can become very slow, due to the very low density of accepting modes with matching frequencies, and therefore cannot be simulated on the time scale accessible to classical MD simulations (e.g., all neat diatomic liquids exhibit VER lifetimes of microseconds or longer[10]).
- A classical description of the relaxing vibrational mode and relevant accepting modes becomes inappropriate and has to be replaced by a consistent quantum treatment of both.

It should be noted that VER via direct energy transfer to the solvent is usually slower than intramolecular energy redistribution (IVR) processes in polyatomic solutes.[45] In such cases, VER to the solvent is usually preceded by a sequence of solvent-assisted IVR steps. At each step, the solute damps the smallest possible amount of energy into the solvent, until the intramolecular mode with the lowest frequency is reached. This gateway mode then damps its energy directly into the solvent. Thus, in polyatomic solutes, the effective frequency may be lower than that of the mode which is originally excited, such that VER is faster and quantum effects are less pronounced.[45]

The perturbative approach provides an alternative framework for the calculation of VER rate constants of high-frequency vibrations.[1,10,46,47] Its starting point is based on the following

* Corresponding author. E-mail: eitan@umich.edu.

10.1021/jp030497+ CCC: $25.00
Published on Web 10/04/2003

general quantum mechanical Hamiltonian of a harmonic vibrational mode coupled to a bath of accepting modes [here, as in the rest of this paper, we use boldface symbols for vectors, and capped symbols (e.g. $\hat{A}$) for operators]:

$$\hat{H} = \hat{H}_s + \hat{H}_b + \hat{H}_{bs} \equiv \hat{H}_0 + \hat{H}_{bs} \tag{1}$$

Here

$$\hat{H}_s = \frac{\hat{p}^2}{2\mu} + \frac{1}{2}\mu\omega^2\hat{q}^2 \tag{2}$$

is the Hamiltonian of the vibrational mode under investigation ($\hat{q}$, $\hat{p}$, μ, and ω are the corresponding coordinate, momentum, reduced mass and frequency, respectively)

$$\hat{H}_b = \sum_{i=1}^{N}\frac{(\hat{P}^{(i)})^2}{2M^{(i)}} + \hat{V}(\hat{Q}^{(1)}, ..., \hat{Q}^{(N)}) = \sum_{i=1}^{N}\frac{(\hat{P}^{(i)})^2}{2M^{(i)}} + \hat{V}(\hat{\mathbf{Q}}) \tag{3}$$

is the Hamiltonian of the bath, which consists of the other intermolecular and intramolecular degrees of freedom [$\hat{\mathbf{Q}} = (\hat{Q}^{(1)}, ..., \hat{Q}^{(N)})$, $\hat{\mathbf{P}} = (\hat{P}^{(1)}, ..., \hat{P}^{(N)})$, $\{M^{(i)}\}$, and $\hat{V}(\hat{\mathbf{Q}}) = \hat{V}(\hat{Q}^{(1)}, ..., \hat{Q}^{(N)})$ are the corresponding coordinates, momenta, masses, and potential energy, respectively], and

$$\hat{H}_{bs} = -\hat{q}\hat{F}(\hat{Q}^{(1)}, ..., \hat{Q}^{(N)}) = -\hat{q}\hat{F}(\hat{\mathbf{Q}}) \tag{4}$$

is the system-bath coupling term. The latter is assumed to be linearized in the vibrational coordinate, $\hat{q}$, which implies that VER takes place via the emission of one vibrational quantum. For simplicity, we assume that the force on the vibrational mode, $\hat{F}(\hat{\mathbf{Q}})$, is a function of only the bath coordinates (the treatment of kinetic coupling terms, which involve momentum-dependent forces, is deferred to the following paper). It should be noted that $\hat{F}(\hat{\mathbf{Q}})$ may be, and often is, a highly nonlinear function of the bath coordinates. The highly nonlinear nature of the force and the large frequency mismatch between the vibrational mode and the majority of the accepting modes, implies that the bath absorbs the energy via a multiphonon-like process.

Given the general Hamiltonian above, the perturbative approach is based on the following three assumptions: (1) *weak system-bath coupling*, to the extent that first-order time-dependent perturbation theory applies; (2) *separation of time scales*, such that the VER lifetime is much longer than the correlation time of the bath-induced force; (3) *the rotating wave approximation (RWA)*, which amounts to the removal of rapidly oscillating terms and decoupling of population relaxation from phase relaxation. Under these conditions, the Bloch Redfield theory (BRT) leads to the following master equation for the vibrational populations:[43,48−58]

$$\frac{d}{dt}P_n = k_{n\leftarrow n+1}P_{n+1} + k_{n\leftarrow n-1}P_{n-1} - (k_{n+1\leftarrow n} + k_{n-1\leftarrow n})P_n \tag{5}$$

Here

$$k_{n\leftarrow n+1} = e^{\beta\hbar\omega}k_{n+1\leftarrow n} = \frac{n+1}{\beta\hbar\omega}\frac{\beta}{2\mu}\tilde{C}(\omega) \tag{6}$$

Here, $\beta = (k_B T)^{-1}$, and

$$\tilde{C}(\omega) = \int_{-\infty}^{\infty} dt\, e^{i\omega t}C(t) \tag{7}$$

is the Fourier transform (FT) of the free bath force−force correlation function (FFCF)

$$C(t) = \langle\delta\hat{F}_0(t)\delta\hat{F}\rangle_0 \tag{8}$$

where $\langle\hat{A}\rangle_0 = \mathrm{Tr}[e^{-\beta\hat{H}_b}\hat{A}]/Z_b$, $Z_b = Tr[e^{-\beta\hat{H}_b}]$, $\delta\hat{F} = \hat{F} - \langle\hat{F}\rangle_0$, and

$$\delta\hat{F}_0(t) = e^{i\hat{H}_b t/\hbar}\delta\hat{F}e^{-i\hat{H}_b t/\hbar} \tag{9}$$

Thus, eq 6 puts the population relaxation rate constants in terms of the FT, at the vibrational frequency, of the quantum-mechanical FFCF, which is evaluated with the vibrational mode frozen at its equilibrium position ($q = 0$).

As is well-known, the population dynamics in eq 5 leads to an exponential decay of the vibrational energy:[55,59,60]

$$\frac{d}{dt}\langle\delta\hat{H}_s\rangle = \sum_{n=0}^{\infty}(n+1/2)\hbar\omega\frac{d}{dt}P_n = -\frac{1}{T_1}\langle\delta\hat{H}_s\rangle \tag{10}$$

Here $\delta\hat{H}_s = \hat{H}_s - \langle\hat{H}_s\rangle_0$, and $\langle\hat{H}_s\rangle_0 = \hbar\omega/2 + \hbar\omega/(e^{\beta p\omega} - 1)$ is the vibrational energy at thermal equilibrium. The central quantity in eq 10 is the VER rate constant, $1/T_1$, which is given by the *Landau−Teller (LT) formula*:[10,46,61]

$$\frac{1}{T_1} = \frac{1 - e^{-\beta\hbar\omega}}{\beta\hbar\omega}\frac{\beta}{2\mu}\tilde{C}(\omega) \tag{11}$$

It should be noted that although $C(t)$ is complex, i.e., $C(t) = C_R(t) + iC_I(t)$ with $C_R(t)$ and $C_I(t)$ the real and imaginary parts, respectively, its FT, $\tilde{C}(\omega)$, is real. Taking advantage of the general symmetries satisfied by $C(t)$, namely $C(-t) = C^*(t)$ and $\tilde{C}(-\omega) = e^{-\beta\hbar\omega}\tilde{C}(\omega)$, the VER rate constant in eq 11 can also be expressed in terms of either the real or imaginary parts of $C(t)$:

$$\frac{1}{T_1} = \frac{\tanh(\beta\hbar\omega/2)}{(\beta\hbar\omega/2)}\frac{\beta}{\mu}\int_0^{\infty} dt\,\cos(\omega t)C_R(t) \equiv -\frac{1}{(\beta\hbar\omega/2)}\frac{\beta}{\mu}\int_0^{\infty} dt\,\sin(\omega t)C_I(t) \tag{12}$$

Thus, $\tilde{C}(\omega)$ can be evaluated from either $C(t)$, $C_I(t)$, or $C_R(t)$.

One difficulty encountered in practical applications of eqs 11 and 12 has to do with the fact that extracting the very small high-frequency Fourier components of the FFCF can become extremely difficult due to statistical noise which accompany real-life simulations. This difficulty is often dealt with by using an extrapolation of the exponential gap law, which usually emerges at low frequencies, to much higher frequencies.[62,63] A similar approach is to combine a short time expansion of the FFCF with a parametrized ansatz that exhibits an exponential gap law behavior at high frequencies, and whose FT can be calculated analytically.[55,64−71]

Another fundamental difficulty is associated with the fact that the input to eqs 11 and 12 consists of the *quantum-mechanical* FFCF, rather than the *classical* FFCF. Unfortunately, the exact calculation of real-time quantum-mechanical correlation functions for general many-body systems remains far beyond the reach of currently available computer resources, due to the exponential scaling of the computational effort with the number of degrees of freedom (DOF).[72] The most popular approach for dealing with this difficulty is to first evaluate the FT of the classical FFCF, and then multiply the result by a frequency-dependent *quantum correction factor* (QCF), $A_Q(\omega)$:[1,47,60,73−86]

$$\tilde{C}(\omega) \approx A_Q(\omega)\tilde{C}^{Cl}(\omega) \tag{13}$$

TABLE 1: Commonly Used Quantum Correction Factors

name	$A_Q(\omega)$	assumption	refs
standard	$2/(1+e^{-\beta\hbar\omega})$	$Re[C(t)] \approx C^{Cl}(t)$	1, 80, 82
harmonic	$\beta\hbar\omega/(1+e^{-\beta\hbar\omega})$	one-phonon process in harmonic bath	60, 79, 80, 81
Schofield	$e^{\beta\hbar\omega/2}$	$C(t) \approx C^{Cl}(t+i\hbar\beta/2)$	84
Egelstaff	$(e^{\beta\hbar\omega/2}/\tilde{C}^{Cl}(\omega)\int_{-\infty}^{\infty} dt\, e^{i\omega t}C^{Cl}(\sqrt{t^2+(\beta\hbar/2)^2})$	$C(t) \approx C^{Cl}(\sqrt{t(t+i\beta\hbar/2)})$	47, 64, 80, 85, 86
harmonic/Schofield	$\sqrt{A_Q^{harmonic}(\omega)A_Q^{Schofield}(\omega)}$	multiphonon process in harmonic bath	73, 75, 78

Here, $\tilde{C}^{Cl}(\omega) = \int_{-\infty}^{\infty} dt\, e^{i\omega t}C^{Cl}(t)$, where $C^{Cl}(t) = \langle dF_0(t)\delta F\rangle_0^{Cl}$ is the *classical* FFCF ($\langle\cdots\rangle_0^{Cl}$ corresponds to averaging over the classical Boltzmann phase space distribution, and the time evolution of $\delta F_0(t)$ is governed by classical mechanics). The important point is that $C^{Cl}(t)$ can be evaluated with relative ease from classical MD simulations. It should be noted that eq 13 amounts to nothing more than a reformulation of the original problem, since knowledge of the exact QCF, $A_Q(\omega)$, is equivalent to, and as difficult to obtain as, the exact quantum mechanical FFCF. However, educated guesses of $A_Q(\omega)$ can be introduced, which are based on the general properties of quantum correlation functions (e.g., detailed balance) and/or the knowledge of what $A_Q(\omega)$ looks like in the very few cases where it can be obtained explicitly. Table 1 lists some of the more popular QCFs. However, estimates provided by the various QCFs can differ by orders of magnitude, and particularly so when high-frequency vibrations are involved.[73,75,83] For example, Egorov et al. have recently estimated $1/T_1$ for O_2 in liquid O_2, at 70 K, and found the following spread of values that were based on different QCFs: 0.00095 (standard), 0.015 (harmonic), 270 (Egelstaff), and 4030 s^{-1} (Schofield). (The experimental value under these conditions is $1/T_1 = 360\ s^{-1}$.) Similar disparities have also been observed in other systems.[77,83]

Several strategies have been proposed in order to address the challenge of providing an effective, computationally feasible, and versatile approximate method for calculating quantum-mechanical real-time correlation functions. These methods are based on various approaches, including a mixed quantum-classical treatment,[87−92] analytical continuation,[66,93−99] centroid molecular dynamics (CMD),[44,100−123] quantum mode coupling theory,[124−126] and the semiclassical (SC) approximation.[72,127−145] These methods have been applied, with relative success, to a rather extensive set of systems and processes. However, the application of these methods to VER in condensed-phase systems has been rather limited. A CMD-based approach for calculating VER rate constants has been pursued by Voth and co-workers[44] and Poulsen and co-workers.[66,120,121] The application of CMD to VER is complicated by the fact that the force in the FFCF is highly nonlinear in the bath coordinates. Hence, these applications of CMD for calculating the FFCF have been based on additional approximations whose validity is not always clear. Applications of the CMD-based approach to model systems have been rather successful, although further tests will be required in order to establish the general applicability of this approach. Rabani and Reichman have proposed a method which is based on computing the coefficients in the short time expansion of the FFCF via imaginary-time path integral simulations.[71] This method has been applied, with relative success, to the case of exponential coupling to a harmonic bath. Here too, further testing on more realistic systems will be required in order to establish the general applicability of this approach.

In the present paper, we consider the application of the linearized-semiclassical initial-value-representation (LSC−IVR) approximation for calculating the quantum-mechanical FFCF. The LSC−IVR approximation has been recently derived by Miller and co-workers,[127,136,142,146−149] by linearizing the forward−backward action in the semiclassical[72,127−145,150−158] initial value representation[130−133,144,159−166] expression for a real-time quantum-mechanical correlation function, with respect to the difference between the forward and backward trajectories. The resulting LSC−IVR approximation for a real time correlation function was found to have the following form:

$$\mathrm{Tr}(e^{-\beta\hat{H}}e^{i\hat{H}t/\hbar}\hat{B}e^{-i\hat{H}t/\hbar}\hat{A}) \approx \frac{1}{(2\pi\hbar)^f}\int d\mathbf{q}_0\int d\mathbf{p}_0(\hat{A}e^{-\beta\hat{H}})_W(\mathbf{q}_0,\mathbf{p}_0)B_W(\mathbf{q}_t^{(Cl)},\mathbf{p}_t^{(Cl)}) \quad (14)$$

Here, f is the number of DOF, $\mathbf{q_0} = (q_0^{(1)}, ..., q_0^{(f)})$ and $\mathbf{p_0} = (p_0^{(1)}, ..., p_0^{(f)})$ are the corresponding coordinates and momenta

$$A_W(\mathbf{q}_0,\mathbf{p}_0) = \int \mathbf{d}\Delta e^{-ip_0\Delta/\hbar}\langle \mathbf{q}_0 + \Delta/2|\,\hat{A}\,|\mathbf{q}_0 - \Delta/2\rangle \quad (15)$$

is the Wigner transform of $\hat{A}$ [with $\Delta = (\Delta^{(1)}, ..., \Delta^{(f)})$],[167,168] and $\mathbf{q}_t^{(Cl)} = \mathbf{q}_t^{(Cl)}(\mathbf{q_0},\mathbf{p_0})$ and $\mathbf{p}_t^{(Cl)} = \mathbf{p}_t^{(Cl)}(\mathbf{q_0},\mathbf{p_0})$ are propagated classically with the initial conditions $\mathbf{q_0}$ and $\mathbf{p_0}$. We have recently shown that the very same approximation can also be derived by linearizing the *exact* real-time path integral expression for the correlation function.[169] More specifically, we showed that it is possible to derive eq 14 without explicitly invoking the semiclassical approximation.

It should be noted that the Wigner representation has been considered by many workers in the past as a convinient starting point for developing approximate treatments of quantum statics and dynamics.[167,168,170−174] In fact, the LSC−IVR approximation of eq 14 can be obtained from the general theory of Wigner distributions via the following straightforward procedure:

$$\mathrm{Tr}(e^{-\beta\hat{H}}e^{i\hat{H}t/\hbar}\hat{B}e^{-i\hat{H}t/\hbar}\hat{A}) = \frac{1}{(2\pi\hbar)^f}\int d\mathbf{q}_0\int d\mathbf{p}_0\,[\hat{A}e^{-\beta\hat{H}}]_W(\mathbf{q_0},\mathbf{p_0})[e^{i\hat{H}t/\hbar}\hat{B}e^{-i\hat{H}t/\hbar}]_W(\mathbf{q_0},\mathbf{p_0}) \approx \frac{1}{(2\pi\hbar)^f}\int d\mathbf{q}_0\int d\mathbf{p}_0\,[\hat{A}e^{-\beta\hat{H}}]_W(\mathbf{q_0},\mathbf{p_0})B_W(\mathbf{q}_t^{(Cl)},\mathbf{p}_t^{(Cl)}) \quad (16)$$

The first equality in eq 16 is exact, and the second is based on the $\hbar \to 0$ limit of the equation of motion of $[e^{i\hat{H}t/\hbar}\hat{B}e^{-i\hat{H}t/\hbar}]_W$. However, the above procedure may appear somewhat arbitrary in the sense that $[\hat{A}e^{-\beta\hat{H}}]_W(\mathbf{q_0},\mathbf{p_0})$ is treated exactly to all orders of $\hbar$, while $[e^{i\hat{H}t/\hbar}\hat{B}e^{-i\hat{H}t/p}]_W$ is replaced by its $\hbar \to 0$ limit. In this respect, the derivation via the linearization of the forward−backward action appears to provide a more consistent route to eq 14.

The major advantage of LSC−IVR has to do with its computational feasibility (although the computation of the Wigner transform in systems with many DOF is not trivial[127]). The approximation also has the attractive features of being exact at the initial time, at the classical limit, and for harmonic systems. Its main disadvantage has to do with the fact that it

can only capture quantum dynamical effects that arise from short-time interferences between the various trajectories (the longer time dynamics is purely classical).[146] However, it should be noted that in condensed phase in general, and in the case of high-frequency VER in particular, the quantities of interest are often dominated by the short-time dynamics of the correlation functions.

In the present paper, we introduce a general semiclassical theory of VER in the condensed phase which is based on the LSC−IVR approximation. A general LSC−IVR-based method for calculating VER rate constants in condensed-phase systems is described in section 2. The application of the method is demonstrated on several model systems in section 3. The results are discussed and summarized in section 4.

II. A Semiclassical Theory of Vibrational Energy Relaxation

The LSC−IVR approximation, eq 14, of the quantum-mechanical FFCF, eq 8, assumes the following form:

$$C(t) \approx \frac{1}{Z_b}\frac{1}{(2\pi\hbar)^N}\int d\mathbf{Q}_0 \int d\mathbf{P}_0\, [\delta\hat{F} e^{-\beta\hat{H}_b}]_W(\mathbf{Q}_0,\mathbf{P}_0)\delta F_W(\mathbf{Q}_t^{(Cl)},\mathbf{P}_t^{(Cl)}) \tag{17}$$

Here

$$\delta F_W(\mathbf{Q}_t^{(Cl)},\mathbf{P}_t^{(Cl)}) = \delta F(\mathbf{Q}_t^{(Cl)}) \tag{18}$$

and

$$[\delta\hat{F} e^{-\beta\hat{H}_b}]_W(\mathbf{Q}_0,\mathbf{P}_0) = \int \mathbf{d}\Delta e^{-i\mathbf{P}_0\Delta/\hbar}\langle \mathbf{Q}_0 + \Delta/2|\, e^{-\beta\hat{H}_b}|\mathbf{Q}_0 - \Delta/2\rangle \delta F(\mathbf{Q}_0 + \Delta/2) \tag{19}$$

A direct calculation of the correlation function in eq 17, in the case of an anharmonic many-body system, would require the calculation of the multidimensional Wigner phase-space integral in eq 19. Unfortunately, it is extremely difficult to perform this calculation via conventional Monte Carlo (MC) techniques, due to the oscillatory phase factor, $e^{-i\mathbf{P}_0\Delta/\hbar}$, in the integrand (the origin of this problem is the same as that of the "sign-problem" encountered in the calculation of real-time path integrals).

One way of overcoming this problem is by introducing an approximation that will allow us to perform the integral in eq 19 analytically. To this end, consider the quadratic expansion of the potential energy of the bath, $V(\mathbf{Q})$ (cf. eq 3), around an arbitrary point $\mathbf{Q} = \mathbf{Q_0}$:

$$V(\mathbf{Q}) \approx V(\mathbf{Q_0}) + \sum_{k=1}^{N}\left.\frac{\partial V}{\partial Q^{(k)}}\right|_{\mathbf{Q}=\mathbf{Q_0}}[Q^{(k)} - Q_0{}^{(k)}] + \frac{1}{2}\sum_{k=1}^{N}\sum_{l=1}^{N}\left.\frac{\partial^2 V}{\partial Q^{(k)}\partial Q^{(l)}}\right|_{\mathbf{Q}=\mathbf{Q_0}}[Q^{(k)} - Q_0{}^{(k)}][Q^{(l)} - Q_0{}^{(l)}] \tag{20}$$

The quadratic term in eq 20 is next written in terms of mass-weighted coordinates, $\{\sqrt{M^{(k)}}[Q^{(k)} - Q_0{}^{(k)}]\}$, and Hessian matrix elements

$$\mathscr{H}_{k,l} = \frac{1}{\sqrt{M^{(k)}M^{(l)}}}\left.\frac{\partial^2 V}{\partial Q^{(k)}\partial Q^{(l)}}\right|_{\mathbf{Q}=\mathbf{Q_0}} \tag{21}$$

followed by a transformation to the normal mode representation:

$$\frac{1}{2}\sum_{k=1}^{N}\sum_{l=1}^{N}\left.\frac{\partial^2 V}{\partial Q^{(k)}\partial Q^{(l)}}\right|_{\mathbf{Q}=\mathbf{Q_0}}[Q^{(k)} - Q_0{}^{(k)}][Q^{(l)} - Q_0{}^{(l)}] = \frac{1}{2}\sum_{k=1}^{N}\sum_{l=1}^{N}\mathscr{H}_{k,l}(\sqrt{M^{(k)}}[Q^{(k)} - Q_0{}^{(k)}])(\sqrt{M^{(l)}}[Q^{(l)} - Q_0{}^{(l)}]) = \frac{1}{2}\sum_{k=1}^{N}(\Omega^{(k)})^2[Q_n^{(k)}]^2 \tag{22}$$

In eq 22

$$Q_n^{(k)} = \sum_{l=1}^{N}T_{l,k}\sqrt{M^{(l)}}[Q^{(l)} - Q_0{}^{(l)}] \tag{23}$$

are the mass-wighted normal mode coordinates, and $\{(\Omega^{(k)})^2\}$ are the eigenvalues of the Hessian matrix, $\{\mathscr{H}_{k,l}\}$. Rewriting the linear term in eq 20 and the kinetic energy of the bath in terms of the normal mode coordinates and momenta yields the following local harmonic approximation (LHA) of the quantum-mechanical bath Hamiltonian around $\mathbf{Q} = \mathbf{Q_0}$:

$$\hat{H}_b \approx \sum_{k=1}^{N}\frac{1}{2}(\hat{P}_n^{(k)})^2 + V(\mathbf{Q_0}) + \sum_{k=1}^{N}G_n^{(k)}\hat{Q}_n^{(k)} + \frac{1}{2}\sum_{k=1}^{N}(\Omega^{(k)})^2[\hat{Q}_n^{(k)}]^2 \tag{24}$$

Here

$$\hat{P}_n^{(k)}(\mathbf{Q_0}) = \sum_{l=1}^{N}T_{l,k}(M^{(l)})^{-1/2}\hat{P}^{(l)} \tag{25}$$

and

$$G_n^{(k)}(\mathbf{Q_0}) = \sum_{l=1}^{N}T_{l,k}(M^{(l)})^{-1/2}\left.\frac{\partial V}{\partial Q^{(l)}}\right|_{\mathbf{Q}=\mathbf{Q_0}} \tag{26}$$

To proceed, we rewrite eq 19 in the following way:

$$[\delta\hat{F} e^{-\beta\hat{H}_b}]_W(\mathbf{Q_0},\mathbf{P_0}) = \langle\mathbf{Q_0}|e^{-\beta\hat{H}_b}|\mathbf{Q_0}\rangle\int \mathbf{d}\Delta e^{-i\mathbf{P_0}\Delta/\hbar}\times \frac{\langle\mathbf{Q_0} + \Delta/2|e^{-\beta\hat{H}_b}|\mathbf{Q_0} - \Delta/2\rangle}{\langle\mathbf{Q_0}|e^{-\beta\hat{H}_b}|\mathbf{Q_0}\rangle}\delta F(\mathbf{Q_0} + \Delta/2) \tag{27}$$

We refrain from applying the LHA to the $\langle\mathbf{Q_0}|e^{-\beta\hat{H}_b}|\mathbf{Q_0}\rangle$ factor preceding the integral (this is essential if the resulting approximation is to yield the correct classical limit and coincide with the exact result at $t = 0$—see below). However, we do apply the LHA of eq 24 to the ratio, $\langle\mathbf{Q_0} + \Delta/2|e^{-\beta\hat{H}_b}|\mathbf{Q_0} - \Delta/2\rangle/\langle\mathbf{Q_0}|e^{-\beta\hat{H}_b}|\mathbf{Q_0}\rangle$. It is important to note that the LHA involves a quadratic expansion only in terms of Δ, while any anharmonicity in terms of $\mathbf{Q_0}$ remains fully accounted for. With the help of the following identity (C is a proportionality constant that does not depend on Q_1 and Q_2)

$$\langle Q_1|e^{-\beta[\hat{P}^2/2 + \Omega^2\hat{Q}^2/2]}|Q_2\rangle = C\exp\left\{-\frac{\Omega}{2\hbar}\frac{1}{\sinh(\beta\hbar\Omega)}\times [\cosh(\beta\hbar\Omega)(Q_1{}^2 + Q_2{}^2) - 2Q_1Q_2]\right\} \tag{28}$$

one can then show that, within the LHA

$$\frac{\langle \mathbf{Q_0}+\Delta/2|e^{-\beta\hat{H}_b}|\mathbf{Q_0}-\Delta/2\rangle}{\langle \mathbf{Q_0}|e^{-\beta\hat{H}_b}|\mathbf{Q_0}\rangle} \approx \exp[-\sum_{j=1}^{N}\alpha^{(j)}(\Delta_n^{(j)}/2)^2] \quad (29)$$

where

$$\Delta_n^{(j)} = \sum_{k=1}^{N} T_{k,j}\sqrt{M^{(k)}}\,\Delta^{(k)} \quad (30)$$

and

$$\alpha^{(j)} = \frac{\Omega^{(j)}}{\hbar}\coth[\beta\hbar\Omega^{(j)}/2] \quad (31)$$

$\alpha^{(j)}$ in eq 31 is real and positive when $[\Omega^{(j)}]^2 > 0$. However, it should be remembered that some of the normal-mode frequencies may be purely imaginary ($[\Omega^{(j)}]^2 < 0$). In such a case, $\Omega^{(j)}$ in eq 31 can be replaced by $i\Omega^{(j)}$, where $\Omega^{(j)}$ is real and positive in the latter. In such a case, $\hbar\alpha^{(j)} \rightarrow \Omega^{(j)}\cot[\beta\hbar\Omega^{(j)}/2]$, which is still real and positive as long as $\beta\hbar\Omega^{(j)} > \pi$. In actual applications, we found that negative values of $\alpha^{(j)}$ are very rare (typically showing up less than once per 1000 randomly sampled configurations). In the applications reported below, it was assumed that such negative values of $\alpha^{(j)}$ can be discarded.

The LHA discussed above is similar to that recently proposed by Ovchinnikov et al. in ref 143. However, the manner in which it is implemented is rather different. More specifically, the LHA is used in ref 143 for calculating the off-diagonal element of the Boltzmann operator, $\langle \mathbf{Q_a}|e^{-\beta\hat{H}}|\mathbf{Q_b}\rangle$, whereas in our case it is used in order to calculate the *ratio* of the off-diagonal and diagonal elements of the Boltzmann operator, $\langle \mathbf{Q_0}+\Delta/2|e^{-\beta\hat{H}_b}|\mathbf{Q_0}-\Delta/2\rangle/\langle \mathbf{Q_0}|e^{-\beta\hat{H}_b}|\mathbf{Q_0}\rangle$ (cf. eq 29). These two versions of the LHA coincide in the case of a fully harmonic system, but are distinctly different otherwise. In fact, applying the LHA to the ratio gives rise to several advantages:

- The approximation that we will obtain below for the FFCF will reproduce the exact classical limit when $\hbar \rightarrow 0$, which would not have been the case if we implemented the LHA as in ref 143.
- The approximation that we will obtain below for the FFCF will be exact at time $t = 0$. This would not have been the case if we utilized the LHA as in ref 143. This may be important since the high-frequency FT components of the FFCF are typically rather sensitive to its behavior at short times.
- Our approach avoids the LHA in the evaluation of $\langle \mathbf{Q_0}|e^{-\beta\hat{H}_b}|\mathbf{Q_0}\rangle$ (see below). In the final result, the initial positions are sampled based on $\langle \mathbf{Q_0}|e^{-\beta\hat{H}_b}|\mathbf{Q_0}\rangle$, such that the anharmonic nature of the potential is fully taken into account (the LHA affects the initial sampling of the momenta though).

To proceed, we will also need to simplify the Δ-dependence of the force, $\delta F(\mathbf{Q_0}+\Delta/2)$. To this end, we assume that $\delta F(\mathbf{Q_0}+\Delta/2)$ can also be approximated by its quadratic expansion, in terms of $\Delta/2$, around $\mathbf{Q} = \mathbf{Q_0}$:

$$\delta F(\mathbf{Q_0}+\Delta/2) \approx \delta F(\mathbf{Q_0}) + \sum_{k=1}^{N} F'_k\frac{\Delta^{(k)}}{2} + \frac{1}{2}\sum_{k=1}^{N}\sum_{l=1}^{N} F''_{k,l}\frac{\Delta^{(k)}}{2}\frac{\Delta^{(l)}}{2}$$

$$= \delta F(\mathbf{Q_0}) + \sum_{k=1}^{N} \tilde{F}'_k\frac{\Delta_n^{(k)}}{2} + \frac{1}{2}\sum_{k=1}^{N}\sum_{l=1}^{N} \tilde{F}''_{k,l}\frac{\Delta_n^{(k)}}{2}\Delta_n^{(l)}2 \quad (32)$$

Here

$$F'_k = \left.\frac{\partial F}{\partial Q^{(k)}}\right|_{\mathbf{Q}=\mathbf{Q_0}};\; F''_{k,l} = \left.\frac{\partial^2 F}{\partial Q^{(k)}\partial Q^{(l)}}\right|_{\mathbf{Q}=\mathbf{Q_0}} \quad (33)$$

and

$$\tilde{F}'_k = \sum_{l=1}^{N}(M^{(l)})^{-1/2}T_{l,k}F'_l;\; \tilde{F}''_{k,l} = \sum_{i=1}^{N}\sum_{j=1}^{N}(M^{(i)}M^{(j)})^{-1/2}T_{i,l}T_{j,k}F''_{i,j} \quad (34)$$

Substituting the approximations in eqs 29 and 32 into eq 19, changing the integration variables from $\{\Delta^{(k)}\}$ to $\{\Delta_n^{(k)}\}$, and performing the Gaussian integral over $\{\Delta_n^{(k)}\}$ analytically yield the following result:

$$[\delta\hat{F}e^{-\beta\hat{H}_b}]_W = \langle \mathbf{Q_0}|e^{-\beta\hat{H}_b}|\mathbf{Q_0}\rangle\prod_{j=1}^{N}\left(\frac{4\pi}{M^{(j)}\alpha^{(j)}}\right)^{1/2}\exp\left[-\frac{(P_{n,0}^{(j)})^2}{p^2\alpha^{(j)}}\right]\times [\delta F(\mathbf{Q_0}) + D(\mathbf{Q_0},\mathbf{P_{n,0}})] \quad (35)$$

Here

$$D(\mathbf{Q_0},\mathbf{P_{n,0}}) = -i\sum_{k=1}^{N}\frac{\tilde{F}'_k P_{n,0}^{(k)}}{\hbar\alpha^{(k)}} + \sum_{k=1}^{N}\frac{\tilde{F}''_{k,k}}{4\alpha^{(k)}} - \sum_{k,l=1}^{N}\frac{\tilde{F}''_{k,l}P_{n,0}^{(k)}P_{n,0}^{(l)}}{2\hbar^2\alpha^{(k)}\alpha^{(l)}} \quad (36)$$

Substituting eq 35 back into eq 17 and changing the integration variables from $\{P_0^{(k)}\}$ to $\{P_{n,0}^{(k)}\}$ then lead to the final form of our approximate expression for the quantum-mechanical FFCF:

$$C(t) \approx \int d\mathbf{Q_0}\frac{\langle \mathbf{Q_0}|e^{-\beta\hat{H}_b}|\mathbf{Q_0}\rangle}{Z_b}\int d\mathbf{P_{n,0}}\prod_{j=1}^{N}\left(\frac{1}{\alpha^{(j)}\pi\hbar^2}\right)^{1/2}\times \exp\left[-\frac{(P_{n,0}^{(j)})^2}{\hbar^2\alpha^{(j)}}\right][\delta F(\mathbf{Q_0}) + D(\mathbf{Q_0},\mathbf{P_{n,0}})]\delta F(\mathbf{Q}_t^{(Cl)}) \quad (37)$$

[Note that the Jacobians involved in the two changes of integration variables, $\Delta \rightarrow \Delta_n$ and $\mathbf{P_0} \rightarrow \mathbf{P_{n,0}}$, are $(\prod_{k=1}^{N} M^{(k)})^{-1/2}$ and $(\prod_{k=1}^{N} M^{(k)})^{1/2}$, respectively, and therefore cancel each other out]. Below, we will refer to the approximation embodied by eq 37 as the LHA−LSC−IVR approximation.

As noted above, eq 37 is exact at time $t = 0$. To see this, note that the integral over $D(\mathbf{Q_0},\mathbf{P_{n,0}})$ with respect to $\mathbf{P_{n,0}}$ vanishes at $t = 0$. The only term left is $[\delta F(\mathbf{Q_0})]^2$, which upon integration over $\mathbf{Q_0}$ yields the exact result:

$$\frac{1}{Z_b}\int d\mathbf{Q_0}\langle \mathbf{Q_0}|e^{-\beta\hat{H}_b}|\mathbf{Q_0}\rangle[\delta F(\mathbf{Q_0})]^2 = \frac{1}{Z_b}\int d\mathbf{Q_0}\langle \mathbf{Q_0}|\, e^{-\beta\hat{H}_b}[\delta\hat{F}]^2|\mathbf{Q_0}\rangle = \frac{\mathrm{Tr}(e^{-\beta\hat{H}_b}[\delta\hat{F}]^2)}{\mathrm{Tr}(e^{-\beta\hat{H}_b})} \quad (38)$$

The classical limit of eq 37 also coincides with the exact classical result. To see this note that, in the classical limit, (1) $\langle \mathbf{Q_0}|e^{-\beta\hat{H}_b}|\mathbf{Q_0}\rangle/Z_b \rightarrow e^{-V(\mathbf{Q_0})}/\int d\mathbf{Q_0}e^{-V(\mathbf{Q_0})}$, (2) $\alpha^{(j)} \rightarrow 2/\beta\hbar^2$ since $\beta\hbar\Omega^{(j)} \ll 1$, such that $\sum_{j=1}^{N}(P_{n,0}^{(j)})^2/\hbar^2\alpha^{(j)} \rightarrow \beta\sum_{j=1}^{N}(P_{n,0}^{(j)})^2/2 \rightarrow \beta\sum_{j=1}^{N}(P_0^{(j)})^2/2M^{(j)}$, and (3) $D(\mathbf{Q_0},\mathbf{P_{n,0}})$, eq 36, vanishes as $\hbar \rightarrow 0$, so one is left with averaging over the time correlation of the classical forces, $\delta F(\mathbf{Q_0})\delta F(\mathbf{Q}_t^{(Cl)})$.

Quantum effects enter eq 37 in several ways:

• The initial positions are sampled based on the exact quantum probability density

$$\mathrm{Prob}(\mathbf{Q_0}) = \frac{\langle \mathbf{Q_0}|e^{-\beta\hat{H}_b}|\mathbf{Q_0}\rangle}{Z_b} = \frac{\langle \mathbf{Q_0}|e^{-\beta\hat{H}_b}|\mathbf{Q_0}\rangle}{\int \mathbf{dQ_0}\langle \mathbf{Q_0}|e^{-\beta\hat{H}_b}|\mathbf{Q_0}\rangle} \quad (39)$$

• The initial (normal-mode) momenta are sampled based on a nonclassical probability density

$$\mathrm{Prob}(\mathbf{P}_{n,0}) = \prod_{j=1}^{N}\left(\frac{1}{\alpha^{(j)}\pi\hbar^2}\right)^{1/2}\exp\left[-\frac{(P_{n,0}^{(j)})^2}{\hbar^2\alpha^{(j)}}\right] \quad (40)$$

It should be noted that $\{\alpha^{(j)}\}$ and therefore $\mathrm{Prob}(\mathbf{P}_{n,0})$ depend parametrically on $\mathbf{Q_0}$.

• The term $D(\mathbf{Q_0},\mathbf{P}_{n,0})$, eq 36, vanishes at the classical limit and has no classical analogue. It represents a purely quantum-mechanical effect that originates from the fact that $\hat{F}$ does not commute with $\hat{H}_b$, such that $(\hat{F}e^{-\beta\hat{H}_b})_W \neq (\hat{F})_W(e^{-\beta\hat{H}_b})_W$. One may therefore view this purely quantum-mechanical term as representing the delocalized nature of the force at $t = 0$. We will therefore refer to its contribution to eq 37 as the *delocalized term*.

It should be noted that the above-mentioned quantum effects include $\hbar$ to all orders [to this end, note that $\alpha^{(j)} = \Omega^{(j)}\coth[\beta\hbar\Omega^{(j)}/2]/\hbar$, eq 31]. This should be contrasted with the quantum corrections that would result from expanding the quantum-mechanical FFCF in powers of $\hbar$, to the first nonvanishing order (for example, see ref 172).

It is also important to note that since $D(\mathbf{Q_0},\mathbf{P}_{n,0})$ is complex, so is the LHA−LSC−IVR FFCF in eq 37. The latter also satisfies the fundamental quantum-mechanical identity $C(-t) = C^*(t)$, which implies that its Fourier transform, $\tilde{C}(\omega)$, is real. This can be seen by using classical-like time reversal symmetry. More specifically, any forward classical trajectory that starts at $\{\mathbf{Q_0},\mathbf{P}_{n,0}\}$ at time 0, and ends at $\{\mathbf{Q}_t,\boldsymbol{P}_{n,t}\}$ at time t, may be *reversed* by starting with $\{\mathbf{Q}_t, -\boldsymbol{P}_{n,t}\}$ at time t, propagating *backward* in time, and ending at $\{\mathbf{Q_0}, -\mathbf{P}_{n,0}\}$ at time 0. The latter trajectory is in turn equivalent to starting at $\{\mathbf{Q_0}, -\mathbf{P}_{n,0}\}$, propagating *backward* in time, and ending at $\{\boldsymbol{Q}_{-t} = \mathbf{Q}_t,\boldsymbol{P}_{n,-t} = -\boldsymbol{P}_{n,t}\}$. Although the sampling of $\mathbf{P}_{n,0}$ in eq 37 is nonclassical, the underlying probability density is still an even function of $\mathbf{P}_{n,0}$, and therefore independent of its sign. This implies that the contributions of the forward and backward trajectories have the same statistical weight, and that the terms in the integrand which are even functions of $\mathbf{P}_{n,0}$ will be symmetrical with respect to time reversal, while terms which are odd functions of $\mathbf{P}_{n,0}$ will be anti-symmetrical with respect to time reversal. The real and imaginary parts in eq 37 are even and odd functions of $\mathbf{P}_{n,0}$, respectively, such that $C(-t) = C^*(t)$.

Finally, it is also important to note that the approximate LHA−LSC−IVR FFCF in eq 37 *does not* rigorously satisfy another fundamental quantum-mechanical identity, namely: $\tilde{C}(-\omega) = e^{-\beta p\omega}\tilde{C}(\omega)$. As a result, substituting the FFCF in eq 37 into eqs 11 and 12 will generally lead to different results. However, it should be noted that the imaginary part of the FFCF in eq 37 emerges from the first-order term in the quadratic expansion of the force in eq 32, whereas the real part originates from the zero and second-order terms in the same expansion. Thus, one anticipates that eq 37 provides a better approximation for $C_R(t)$ in comparison to $C_I(t)$, and that the best approximation for the VER rate constant will be obtained by substituting the *real part* of the FFCF in eq 37, into the first equality in eq 12. Substituting the *imaginary part* of the FFCF in eq 37, into the second equality in eq 12, is expected to yield a less accurate approximation. Finally, substituting the complex FFCF in eq 37, into eq 11, is expected to yield an approximation whose quality is intermediate between these two extremes. This trend is indeed observed in the examples considered below.

Equation 37 represents the main result of this paper and gives rise to the following algorithm for calculating the (approximate) quantum-mechanical FFCF:

1. Sample $\mathbf{Q_0}$, with the probability density of eq 39, via an imaginary-time path integral molecular-dynamics or Monte Carlo simulation (PIMD and PIMC respectively),[175,176] and calculate $F(\mathbf{Q_0})$.

2. Perform a LHA around each value of $\mathbf{Q_0}$, find the normal-mode frequencies, $\{\Omega^{(k)}\}$, and transformation matrix, $\{T_{k,l}\}$, and evaluate $\{\alpha^{(k)}\}$, $\{\tilde{F}'_k(\mathbf{Q_0})\}$ and $\{\tilde{F}''_{k,l}(\mathbf{Q_0})\}$. The Jacobi method[177] has been used for diagonalizing the Hessian matrix in the applications reported below.

3. MC Sample the initial (normal-mode) momenta, $\{P_{n,0}^{(k)}\}$, based on the Gaussian probability density in eq 40.

4. Calculate $\mathbf{Q}_t^{(Cl)}$ via a classical MD simulation, for each set of initial positions and momenta, $\mathbf{Q_0}$ and $\mathbf{P}_{n,0}$, and time correlate $\delta F(\mathbf{Q}_t^{(Cl)})$ with $\delta F(\mathbf{Q_0})$ and $D(\mathbf{Q_0},\mathbf{P}_{n,0})$.

In the next section, we present the results of calculations based on the application of this algorithm to several model systems.

III. Applications

A. Exponential Coupling to a Harmonic Bath. The first model that we consider involves a bath consisting of uncoupled harmonic oscillators of different frequencies

$$\hat{H}_b = \sum_{j=1}^{N}\left(\frac{(\hat{P}^{(j)})^2}{2M^{(j)}} + \frac{1}{2}M^{(j)}(\omega^{(j)})^2(\hat{Q}^{(j)})^2\right) \quad (41)$$

and a force which is exponential in the bath coordinates:

$$\hat{F}(\hat{\mathbf{Q}}) = e^{R(\hat{\mathbf{Q}})} \quad (42)$$

where

$$R(\hat{\mathbf{Q}}) = \sum_j c^{(j)}\sqrt{\frac{2M^{(j)}\omega^{(j)}}{\hbar}}\,\hat{Q}^{(j)} \quad (43)$$

The fact that the exact quantum-mechanical FFCF can be obtained analytically for this model[63] has established it as a convenient benchmark.[71,83] The exact quantum-mechanical FFCF is given by

$$C(t) = e^{B(0)}(e^{B(t)} - 1) \quad (44)$$

where

$$B(t) = \langle \hat{R}_0(t)\hat{R}(0)\rangle_0 = \int_0^\infty d\omega\Gamma(\omega)\{[n(\omega)+1]e^{-i\omega t} + n(\omega)e^{i\omega t}\} \quad (45)$$

$$\Gamma(\omega) = \sum_k (c^{(k)})^2\delta(\omega - \omega^{(k)}) \quad (46)$$

and $n(\omega) = [\exp(\beta\hbar\omega) - 1]^{-1}$.

It should be noted that the LSC−IVR expression in eq 14 is exact when the system is harmonic, regardless of whether the operators in the correlation function are linear in the system coordinates and/or momenta. Thus, for this model, the FFCF

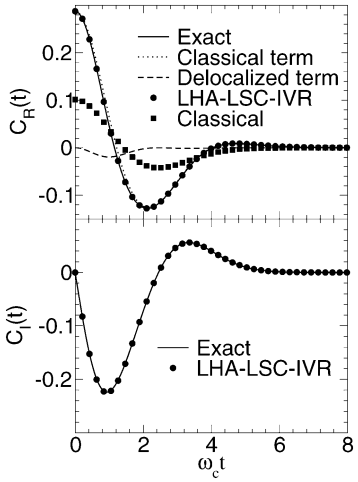

Figure 1. Real and imaginary parts of the LHA−LSC−IVR FFCF, for the case of exponential coupling to a harmonic bath. The exact and classical results are shown for reference. The contributions of the classical and delocalized initial force terms to the real part are also shown.

in eq 17 actually coincides with the exact FFCF, eq 44. However, our LHA−LSC−IVR working expression, eq 37, also involves an approximate quadratic expansion of $\delta F(\mathbf{Q_0} + \Delta/2)$ (cf. eq 32). The above model therefore provides a convenient way of testing this approximation. In fact, the fact that the system is harmonic allows for the analytical calculation of the FFCF in eq 37. The final result can be written in the following form:

$$C(t) \approx e^{B_R(0)}\left[(e^{B_R(t)} - 1) + ie^{B_R(t)}B_I(t) - \frac{1}{2}e^{B_R(t)}B_I^2(t)\right] \quad (47)$$

Here $B_R(t)$ and $B_I(t)$ are the real and imaginary parts of $B(t)$, respectively (cf. eq 45). Interestingly, eq 47 can be obtained from the exact eq 44 via a second-order expansion in terms of $B_I(t)$.

The real and imaginary parts of the exact (eq 44) and approximate (eq 47) FFCF for this model are shown in Figure 1. The calculations were performed with a spectral density of the following form:

$$\Gamma(\omega) = 2\lambda\frac{\omega^\alpha}{\omega_c^{\alpha+1}}\exp\left(-\frac{\omega^2}{\omega_c^2}\right) \quad (48)$$

and for the following values of the parameters: $\lambda = 0.20$, $\alpha = 3$ and $\beta\hbar\omega_c = 4.0$. The approximate real and imaginary parts are found to be in excellent agreement with the exact result. We also compare the contributions of the two terms that constitute the real part of the FFCF in eq 47, namely $e^{B_R(0)}(e^{B_R(t)} - 1)$ (the "classical term") and $-e^{B_R(t)}e^{B_R(0)}C_I^2(t)/2$ (the "delocalized term"). It should be noted that the first term arises from the classical force at $t = 0$, $\delta F(\mathbf{Q_0})$, while the second term arises from the purely quantum mechanical term, $D(\mathbf{Q_0},\mathbf{P}_{n,0})$ (cf. eq 37). Neglecting the latter implies initial sampling based on the Wigner transform of the Boltzmann operator, $e^{-\beta\hat{H}_b}$, and not accounting for delocalization in the evaluation of the force at $t = 0$. Figure 1 clearly indicates that the time-domain behavior of the real part is dominated by the classical term. It should also be noted that the imaginary part in Figure 1, which is purely quantum-mechanical, is completely determined by the delocalized term.

The FT of the exact (eq 44), and approximate (eq 47), FFCFs are shown in Figure 2 on a semilog plot. The approximate FT

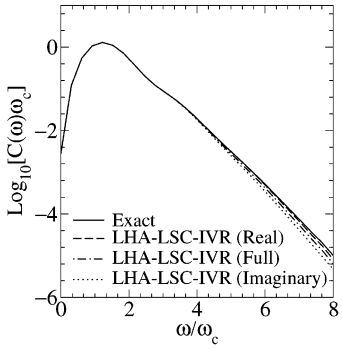

Figure 2. Semilog plot of the FT of the exact (eq 44), and approximate (eq 47) FFCF, for the case of exponential coupling to a harmonic bath. The approximate FT of the FFCF is given as obtained from the full, real part and imaginary part of the FFCF in eq 47.

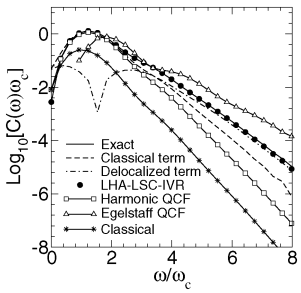

Figure 3. Contributions of the classical and delocalized terms, for the case of exponential coupling to a harmonic bath. It should be noted that the contribution of the delocalized term switched sign from negative at low frequencies to positive at high frequencies. Thus, what is actually plotted is the logarithm of the absolute value of this contribution. Also shown are the classical results and predictions based on the harmonic and Egelstaff QCFs.

of the FFCF is given as obtained from the full, real part and imaginary part of the FFCF in eq 47 [for the exact FFCF, $\tilde{C}(\omega) = 4\int_0^\infty dt\ \cos(\omega t)C_R(t)/(1 + e^{-\beta\hbar\omega}) = -4\int_0^\infty dt\ \sin(\omega t)C_I(t)/(1 - e^{-\beta\hbar\omega})$]. As expected, the best agreement with the exact result is obtained when the FT is calculated from the real part of the FFCF in eq 47. The agreement is excellent in this case, and the approximation essentially coincides with the exact result. Deviations from the exact result are observed when the full FFCF is used, and even more so when the imaginary part of the FFCF is used. However, even then, the predictions are found to be in very good agreement with the exact results.

In Figure 3, we compare the contributions of the above-mentioned classical and delocalized contributions to the FT of the FFCF (as obtained from the real part of the FFCF). Unlike the behavior in the time domain, the results in Figure 3 clearly show that neglecting the delocalized term leads to rapid deterioration in the quality of the approximation as the frequency increases. In fact, this purely quantum-mechanical term, which is rather small at low frequencies, becomes dominant at high frequencies! This observation provides a rather unique perspective on the origin of the quantum enhancement of high-frequency VER rate constants and points to force delocalization, rather than nonclassical phase-space sampling, as its origin. In Figure 3, we also show the predictions obtained by using classical mechanics, which deviate by orders of magnitude from the exact results at high frequencies. We also show the predictions of the best performing harmonic and Egelstaff QCFs[83] (cf. Table 1). The predictions obtained via these QCFs are seen to differ from one another by orders of magnitude at high frequencies, and the agreement of neither of them with the exact result is as good as that obtained via LHA−LSC−IVR. It should also be

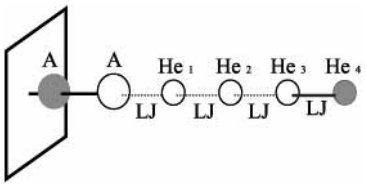

Figure 4. Schematic view of the linear helium cluster model.

noted that none of the QCFs provide accurate predictions in the time and frequency domain, simultaneously,[83] while the predictions of LHA−LSC−IVR are in excellent agreement with the exact results in both cases.

B. A Linear Helium Cluster. The second model to be considered has been recently used by Poulsen and co-workers[66,120,121] in order to examine the performance of another CMD-based method for calculating the quantum-mechanical FFCF. In this model, a harmonic diatomic molecule, A_2, is attached to a wall, and held fixed perpendicular to it (cf. Figure 4). The A atom which is not attached to the wall is coupled to a short linear chain of four helium atoms, with the last helium atom held in place. The interaction between the A atom and the helium atom next to it, as well as the interactions between the helium atoms, are described by anharmonic Lennard-Jones (LJ) potentials, which mimic realistic liquid-phase interactions. Only nearest neighbor interactions are taken into account.

The A_2 molecule and helium chain are assumed to lie along the x axis, with the origin positioned on the A atom which is attached to the wall. The second A atom is positioned at $x_0 = r_{eq} + \delta_0$, where r_{eq} is the equilibrium bond length of A_2 and δ_0 is the deviation relative to it. The positions of helium atoms 1, 2 and 3 are given by $x_1 = r_{eq} + \sigma_{He-A} + \delta_1$, $x_2 = r_{eq} + \sigma_{He-A} + \sigma_{He-He} + \delta_2$, and $x_3 = r_{eq} + \sigma_{He-A} + 2\sigma_{He-He} + \delta_3$ respectively, where σ_{He-A} and σ_{He-He} are the familiar LJ parameters. The position of the last helium atom is fixed at $x_4 = r_{eq} + \sigma_{He-A} + 3\sigma_{He-He}$. The overall potential energy of this system is given by

$$V(\delta_0,\delta_1,\delta_2,\delta_3) = \frac{1}{2}\mu\omega^2{\delta_0}^2 + V_{LJ}^{He-A}(\sigma_{He-A} + \delta_1 - \delta_0) + V_{LJ}^{He-He}(\sigma_{He-He} + \delta_2 - \delta_1) + V_{LJ}^{He-He}(\sigma_{He-He} + \delta_3 - \delta_2) + V_{LJ}^{He-He}(\sigma_{He-He} - \delta_3) \quad (49)$$

where $V_{LJ}(r) = 4\epsilon[(\sigma/r)^{12} - (\sigma/r)^6]$. The parameters used are the same as these in ref 120: $\sigma_{He-A} = 4.944$ au, $\sigma_{He-He} = 4.310$ au, $\epsilon_{He-A}/k_B = 25.1$ K, and $\epsilon_{He-He}/k_B = 10.2$ K. The force on the diatomic molecule is obtained by linearizing the potential with respect to the diatomic displacement, δ_0:

$$F = -\left.\frac{\partial V}{\partial \delta_0}\right|_{\delta_0=0} = V'_{LJ}{}^{He-A}(\sigma_{He,A} + \delta_1) \quad (50)$$

The low dimensionality of this system allows for the calculation of the exact quantum mechanical FFCF (the exact results given in ref 120 for the same values of the parameters have been adopted for this purpose). Furthermore, a numerically exact calculation of the Wigner transforms involved in eq 17 via MC sampling is feasible. The real part of the FFCF at 40 K, as obtained for this model by using different methods, is shown in Figure 5. The LSC−IVR FFCF, with or without the LHA, coincides with the exact FFCF at $t = 0$, and captures the exact short time behavior rather well. At the same time, the LSC−IVR and LHA−LSC−IVR FFCFs are seen to decay too fast and are unable to capture the oscillatory behavior of the FFCF at longer times. The latter observation is consistent with

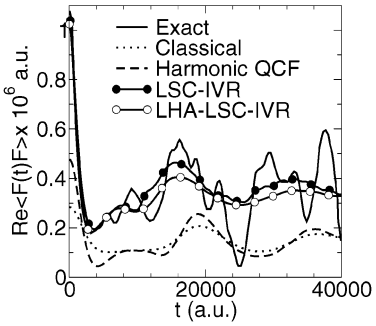

Figure 5. Real part of the (unnormalized) FFCF, as obtained for the helium cluster model. Shown are the exact quantum mechanical result, the classical prediction, and results obtained via LSC−IVR, LHA−LSC−IVR, and the harmonic QCF.

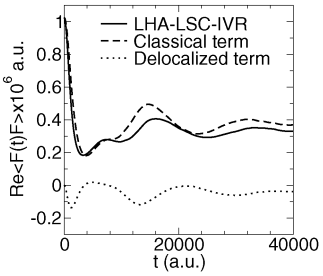

Figure 6. Contributions of the classical and delocalized initial force terms to the FFCF within the helium cluster model.

that made by other authors who attempted to apply LSC−IVR for the calculation of correlation functions in low dimensional systems.[139,146] Although the LHA leads to a somewhat faster decay, the overall temporal behavior of the LHA−LSC−IVR FFCF is rather similar to that of the LSC−IVR FFCF, particularly so at short times. It should be noted that the FFCF in a truly condensed phase system will be characterized by a relatively short correlation time, during which the LHA−LSC−IVR approximation seems to be rather reliable. The classical FFCF and the FFCF obtained by using the harmonic QCF are also shown in Figure 5. The relatively large deviation between the classical and quantum-mechanical FFCFs is indicative of the fact that the "solvent" is pronouncedly quantum-mechanical in this case, as could be expected from helium at 40 K. Figure 5 also demonstrates the failure of the harmonic QCF, which can be attributed to the pronouncedly anharmonic nature of the potential. In Figure 6, we show the contributions of the classical and quantum-mechanical ("delocalized") contributions to the initial force in the LHA−LSC−IVR FFCF. The classical contribution is seen to dominate, although the delocalized contribution is significant. It should be remembered however that considering the contributions of these two terms in the time domain is probably misleading and that the purely quantum mechanical delocalized term was seen to dominate the high-frequency FT of the FFCF in all the other model systems that we have studied (cf. sections 3.A and 3.C).

C. A Diatomic Solute in a Monatomic Solvent (Breathing Sphere Model). We next consider the VER of a diatomic solute in a monatomic solvent. The vibrational mode is assumed to have a spherical symmetry, and can therefore be viewed as a "breathing sphere".[55,178,179] The solute−solvent and solvent−solvent interactions are treated in terms of spherically symmetric pair potentials. The overall potential energy is given by

$$V = \frac{1}{2}\mu\omega^2 q^2 + \sum_{j<k}\phi_s(r_{jk}) + \sum_j \phi(r_{j0}, q) \quad (51)$$

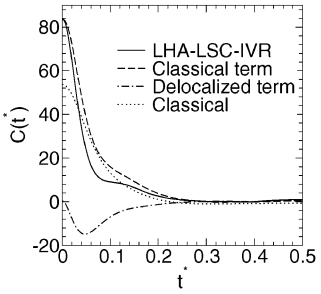

Figure 7. Real part of the FFCF, as obtained for the breathing sphere model. Also shown are the classical FFCF and the contributions of the classical and delocalized initial force terms.

where $\phi_s(r)$ is the solvent−solvent pair potential, $\phi(r, q)$ is the solvent−solute pair potential, r_{jk} is the distance between the jth and kth solvent atoms, and r_{j0} is the distance between the center of mass of the diatomic solute and the jth solvent atom. The force is obtained by the linearization of the potential with respect to q:

$$F = -\left.\frac{\partial V}{\partial q}\right|_{q=0} = -\sum_j \left.\frac{\partial \phi}{\partial q}\right|_{q=0}(r_{j0}) \qquad (52)$$

To enhance the computational feasibility, calculations were performed on a two-dimensional liquid and under the assumption that the solvent atoms and the diatomic solute have the same mass, and that $\phi_s(r)$ and $\phi(r)$ are identical and given by a LJ potential:[180] $\phi_s(r) = \phi(r) = V_{LJ}(r) = 4\epsilon[(\sigma/r)^{12} - (\sigma/r)^6]$. The mass and LJ parameters in the actual simulations were chosen to coincide with these of liquid neon, namely $\sigma = 2.72$ Å and $\epsilon/k_B = 47.0$ K. The calculations reported below were performed on a 2D liquid consisting of 81 atoms confined to a square, at a reduced density and temperature of $\rho^* = 0.70$ and $T^* = 0.68$, respectively. Periodic boundary conditions and a potential cutoff at 3σ have been employed. For reference, we note that the above parameters correspond to a temperature of 32 K and density of 9.46 nm^{-2} in the case of neon.

The real part of the FFCF obtained from eq 37 is compared with the classical FFCF in Figure 7. Since the exact quantum-mechanical result is not known for this case, and experimental results are unavailable for this particular model system, evaluation of the quality of the approximation is difficult. However, the LHA−LSC−IVR FFCF is clearly different from the classical result, thereby suggesting that quantum mechanics imposes pronounced modifications under these conditions. The larger initial value of the LHA−LSC−IVR FFCF, which coincides with the exact quantum-mechanical value, is attributed to the nonclassical initial sampling. In this context, it should be noted that the force is very sensitive to displacements, and especially so if they are associated with sampling the repulsive region of the LJ potential. Also shown in Figure 7 are the contributions to the real part of the FFCF from the classical and delocalized terms to the force at $t = 0$. Although the major contribution is seen to arise from the classical term, the contribution of the delocalized term is by no means negligible.

In Figure 8, we present a semilog plot of the FT of the FFCF, as obtained from the full, real part and imaginary part of the LHA−LSC−IVR FFCF in eq 37. The frequency is given in reduced units (for reference, we note that $\omega^* = 100$ corresponds to 273 cm^{-1} in the case of neon). Very similar predictions are obtained in all three cases. In Figure 9, we compare the classical and delocalized contributions to the FT of the LHA−LSC−IVR FFCF (as obtained from the real part). The delocalized term is once again seen to be the dominant one at high

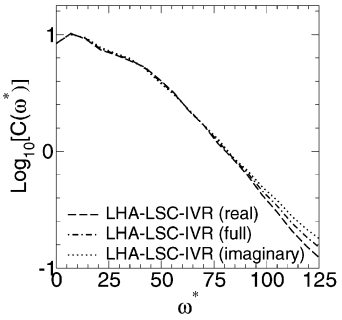

Figure 8. Semilog plot of the FT of the FFCF for the breathing sphere model, as obtained from the full version, real part, and imaginary part of the FFCF in eq 47.

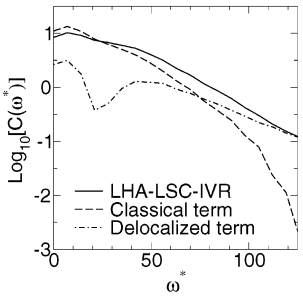

Figure 9. Semilog plot of the classical and delocalized initial force terms to the FT of the FFCF, for the breathing sphere model. It should be noted that the contribution of the delocalized term switched sign from negative at low frequencies to positive at high frequencies. Thus, what is actually plotted is the logarithm of the absolute value of this contribution.

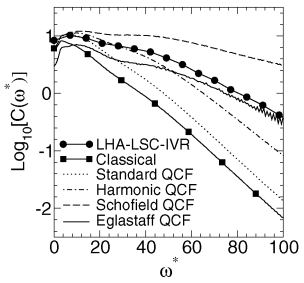

Figure 10. Comparison of the predictions of LHA−LSC−IVR, classical mechanics, and various QCFs for the FT of the FFCF.

frequencies. Finally, a comparison with the predictions based on classical mechanics and various QCFs is shown in Figure 10. The deviation between the classical and LHA−LSC− IVR predictions grows rapidly as the frequency increases, with a significant enhancement of the LHA−LSC−IVR prediction relative to the classical one. It is also seen that the prediction based on the Egelstaff QCF is the closest to that of LHA−LSC−IVR at the high-frequency region. We view this observation as encouraging, since in the past, the Egelstaff QCF has been seen to provide the best predictions in applications to VER. It should also be noted that a direct calculation of the FT at higher frequencies is very difficult due to numerical noise (cf. section 1). However, assuming that the exponential gap law that emerges at the lower frequencies persists, one can estimate the high-frequency FT by extrapolation.

IV. Conclusions

The ability of LSC−IVR to capture quantum effects over a short period of time suggests that it is well suited for estimating relatively short lived quantum-mechanical correlation functions in condensed phase systems. The validity of this hypothesis has

been previously demonstrated in the calculation of reaction rate constants, which depend on the short time dynamics of the flux−flux correlation function.[148,181] In the present paper, we have proposed an LSC−IVR-based method for calculating the quantum-mechanical FFCF and thereby the VER rate constant. It should be noted that the high frequency of most molecular vibrations can lead to deviations by orders of magnitude between the corresponding classical and quantum-mechanical VER rate constants. VER therefore constitutes a prime example for an inherently nonclassical process that takes place in a condensed phase environment. The main obstacle involved in applying LSC−IVR to realistic anharmonic condensed-phase systems originates from the difficulty of calculating multidimensional Wigner transforms. This difficulty has been bypassed in the present study by a new implementation of the LHA, which allows for an analytical calculation of the Wigner integral. Our implementation of the LHA has several important advantages: (1) the approximate FFCF reduces to the exact classical limit as $\hbar \rightarrow 0$; (2) the approximate FFCF is exact at $t = 0$; (3) the sampling over the initial positions in the resulting expression for the FFCF is done on the exact *anharmonic* potential.

The proposed method has been successfully applied to three nontrivial model systems: (1) a vibrational mode coupled to a harmonic bath, with the coupling exponential in the bath coordinates; (2) a diatomic molecule coupled to a short chain of helium atoms that interact via LJ pair potentials; (3) a spherically symmetric diatomic molecule (a "breathing sphere"), in a two-dimensional monatomic LJ liquid. The predicted short-time behavior and high-frequency FT have been found to be in good agreement with the relevant exact results, or their best estimates, thereby providing further evidence for the suitability of the LHA−LSC−IVR approximation for calculating the quantum-mechanical FFCF.

Another advantage of LSC−IVR, beyond providing a reasonable quantitative estimate of the quantum-mechanical FFCF, has to do with its ability to shed light on the origin and significance of the quantum effects. More specifically, we find that the quantum enhancement of the VER rate constant is dominated by a purely quantum mechanical term, which vanishes in the classical limit ($\hbar \rightarrow 0$). This finding calls into question the notion that the quantum-mechanical FFCF can be generally and reliably estimated from the classical FFCF (with the exception of the rather specialized examples in Table 1). Furthermore, LHA−LSC−IVR provide a reasonable starting point for understanding the *quantum-mechanical* mechanism underlying VER in different systems, and answer the important question of how it differs from the corresponding *classical* mechanism. To this end, further development of the theory presented herein will be needed. We take a first step toward this goal in the following paper, by extending the theory and computational scheme to diatomic molecular liquids. The resulting LHA−LSC−IVR-based methodology is then applied to the challenging problem of calculating the extremely slow and highly quantum-mechanical VER rate constant in liquid oxygen. The result is found to be in good agreement with experiment, thereby providing further support for this promising approach to VER.

Acknowledgment. The authors are grateful for financial support from the National Science Foundation through Grant No. CHE-0306695.

References and Notes

(1) Oxtoby, D. W. *Adv. Chem. Phys.* **1981**, *47 (Part 2)*, 487.
(2) Oxtoby, D. W. *Annu. Rev. Phys. Chem.* **1981**, *32*, 77.
(3) Oxtoby, D. W. *J. Phys. Chem.* **1983**, *87*, 3028.
(4) Chesnoy, J.; Gale, G. M. *Ann. Phys. Fr.* **1984**, *9*, 893.
(5) Chesnoy, J.; Gale, G. M. *Adv. Chem. Phys.* **1988**, *70 (Part 2)*, 297.
(6) Harris, C. B.; Smith, D. E.; Russell, D. J. *Chem. Rev.* **1990**, *90*, 481.
(7) Miller, D. W.; Adelman, S. A. *Int. Rev. Phys. Chem.* **1994**, *13*, 359.
(8) Stratt, R. M.; Maroncelli, M. *J. Phys. Chem.* **1996**, *100*, 12981.
(9) Elsaesser, T.; Kaiser, W. *Annu. Rev. Phys. Chem.* **1991**, *42*, 83.
(10) Owrutsky, J. C.; Raftery, D.; Hochstrasser, R. M. *Annu. Rev. Phys. Chem.* **1994**, *45*, 519.
(11) Calaway, W. F.; Ewing, G. E. *J. Chem. Phys.* **1975**, *63*, 2842.
(12) Brueck, S. R. J.; Osgood, R. M. *Chem. Phys. Lett.* **1976**, *39*, 568.
(13) Laubereau, A.; Kaiser, W. *Rev. Mod. Phys.* **1978**, *50*, 607.
(14) Faltermeier, B.; Protz, R.; Maier, M.; Werner, E. *Chem. Phys. Lett.* **1980**, *74*, 425.
(15) Faltermeier, B.; Protz, R.; Maier, M. *Chem. Phys.* **1981**, *62*, 377.
(16) Chateau, M.; Delalande, C.; Frey, R.; Gale, G. M.; Pradère, F. *J. Chem. Phys.* **1979**, *71*, 4799.
(17) Delalande, C.; Gale, G. M. *J. Chem. Phys.* **1980**, *73*, 1918.
(18) Roussignol, P.; Delalande, C.; Gale, G. M. *Chem. Phys.* **1982**, *70*, 319.
(19) Heilweil, E. J.; Doany, F. E.; Moore, R.; Hochstrasser, R. M. *J. Chem. Phys.* **1982**, *76*, 5632.
(20) Heilweil, E. J.; Casassa, M. P.; Cavanagh, R. R.; Stephenson, J. C. *Chem. Phys. Lett.* **1985**, *117*, 185.
(21) Heilweil, E. J.; Casassa, M. P.; Cavanagh, R. R.; Stephenson, J. C. *J. Chem. Phys.* **1986**, *85*, 5004.
(22) Harris, A. L.; Brown, J. K.; Harris, C. B. *Annu. Rev. Phys. Chem* **1988**, *39*, 341.
(23) Paige, M. E.; Russell, D. J.; Harris, C. B. *J. Chem. Phys.* **1986**, *85*, 3699.
(24) Owrutsky, J. C.; Kim, Y. R.; Li, M.; Sarisky, M. J.; Hochstrasser, R. M. *Chem. Phys. Lett.* **1991**, *184*, 368.
(25) Moustakas, A.; Weitz, E. *J. Chem. Phys.* **1993**, *98*, 6947.
(26) Kliner, D. A. V.; Alfano, J. C.; Barbara, P. F. *J. Chem. Phys.* **1993**, *98*, 5375.
(27) Zimdars, D.; Tokmakoff, A.; Chen, S.; Greenfield, S. R.; Fayer, M. D. *Phys. Rev. Lett.* **1993**, *70*, 2718.
(28) Pugliano, N.; Szarka, A. Z.; Gnanakaran, S.; Hochstrasser, R. M. *J. Chem. Phys.* **1995**, *103*, 6498.
(29) Paige, M. E.; Harris, C. B. *Chem. Phys.* **1990**, *149*, 37.
(30) Salloum, A.; Dubost, H. *Chem. Phys.* **1994**, *189*, 179.
(31) Tokmakoff, A.; Sauter, B.; Fayer, M. D. *J. Chem. Phys.* **1994**, *100*, 9035.
(32) Tokmakoff, A.; Fayer, M. D. *J. Chem. Phys.* **1995**, *103*, 2810.
(33) Urdahl, R. S.; Myers, D. J.; Rector, K. D.; Davis, P. H.; Cherayil, B. J.; Fayer, M. D. *J. Chem. Phys.* **1997**, *107*, 3747.
(34) Owrutsky, J. C.; Li, M.; Locke, B.; Hochstrasser, R. M. *J. Phys. Chem.* **1995**, *99*, 4842.
(35) Laenen, R.; Rauscher, C.; Laubereau, A. *Phys. Rev. Lett.* **1998**, *80*, 2622.
(36) Woutersen, S.; Emmerichs, U.; Nienhuys, H.; Bakker, H. J. *Phys. Rev. Lett.* **1998**, *81*, 1106.
(37) Myers, D. J.; Chen, S.; Shigeiwa, M.; Cherayil, B. J.; Fayer, M. D. *J. Chem. Phys.* **1998**, *109*, 5971.
(38) Sagnella, D. E.; Straub, J. E.; Jackson, T. A.; Lim, M.; Anfinrud, P. A. *Proc. Natl. Acad. Sci. U.S.A.* **1999**, *96*, 14324.
(39) Hamm, P.; Lim, M.; Hochstrasser, R. M. *J. Chem. Phys.* **1997**, *107*, 1523.
(40) Brown, J. K.; Harris, C. B.; Tully, J. C. *J. Chem. Phys.* **1988**, *89*, 6687.
(41) Whitnell, R. M.; Wilson, K. R.; Hynes, J. T. *J. Phys. Chem.* **1990**, *94*, 8625.
(42) Whitnell, R. M.; Wilson, K. R.; Hynes, J. T. *J. Chem. Phys.* **1992**, *96*, 5354.
(43) Figueirido, F. E.; Levy, R. M. *J. Chem. Phys.* **1992**, *97*, 703.
(44) Jang, S.; Pak, Y.; Voth, G. A. *J. Phys. Chem. A* **1999**, *103*, 10289.
(45) Deng, Y.; Stratt, R. M. *J. Chem. Phys.* **2002**, *117*, 1735.
(46) Zwanzig, R. *J. Chem. Phys.* **1961**, *34*, 1931.
(47) Berne, B. J.; Jortner, J.; Gordon, R. *J. Chem. Phys.* **1967**, *47*, 1600.
(48) Redfield, A. G. *IBM J.* **1957**, *1*, 19.
(49) Wangsness, R. K.; Bloch, F. *Phys. Rev.* **1953**, *89*, 728.
(50) Slichter, C. P. *Principles of Magnetic Resonance*; Springer-Verlag: Berlin, 1990.
(51) Abragam, A. *The Principles of Nuclear Magnetism*; Oxford: London, 1961.
(52) Jean, J. M.; Friesner, R. A.; Fleming, G. R. *J. Chem. Phys.* **1992**, *96*, 5827.
(53) Gai, H.; Voth, G. A. *J. Chem. Phys.* **1993**, *99*, 740.
(54) Pollard, W. T.; Friesner, R. A. *J. Chem. Phys.* **1994**, *100*, 5054.
(55) Egorov, S. A.; Skinner, J. L. *J. Chem. Phys.* **1996**, *105*, 7047.
(56) Geva, E.; Rosenman, E.; Tannor, D. J. *J. Chem. Phys.* **2000**, *113*, 1380.
(57) Kampen, N. G. V. *Stochastic Processes in Physics and Chemistry*; Elsevier: Amsterdam, 1992.

(58) Shi, Q.; Geva, E. *J. Chem. Phys.* **2003**, *118*, 7562.
(59) Nitzan, A.; Silbey, R. *J. Chem. Phys.* **1974**, *60*, 4070.
(60) Bader, J. S.; Berne, B. J. *J. Chem. Phys.* **1994**, *100*, 8359.
(61) Landau, L.; Teller, E. Z. *Z. Sowjetunion* **1936**, *34*, 10.
(62) Nitzan, A.; Mukamel, S.; Jortner, J. *J. Chem. Phys.* **1974**, *60*, 3929.
(63) Nitzan, A.; Mukamel, S.; Jortner, J. *J. Chem. Phys.* **1975**, *63*, 200.
(64) Everitt, K. F.; Egorov, S. A.; Skinner, J. L. *Chem. Phys.* **1998**, *235*, 115.
(65) Everitt, K. F.; Skinner, J. L. *J. Chem. Phys.* **1999**, *110*, 4467.
(66) Poulsen, J.; Rossky, P. J. *J. Chem. Phys.* **2001**, *115*, 8014.
(67) Douglass, D. C. *J. Chem. Phys.* **1961**, *35*, 81.
(68) Adelman, S. A.; Stote, R. H. *J. Chem. Phys.* **1988**, *88*, 4397.
(69) Stote, R. H.; Adelman, S. A. *J. Chem. Phys.* **1988**, *88*, 4415.
(70) Adelman, S. A.; Muralidhar, R.; Stote, R. H. *J. Chem. Phys.* **1991**, *95*, 2738.
(71) Rabani, E.; Reichman, D. R. *J. Phys. Chem. B* **2001**, *105*, 6550.
(72) Makri, N. *Annu. Rev. Phys. Chem.* **1999**, *50*, 167.
(73) Egorov, S. A.; Everitt, K. F.; Skinner, J. L. *J. Phys. Chem. A* **1999**, *103*, 9494.
(74) Egorov, S. A.; Skinner, J. L. *J. Chem. Phys.* **2000**, *112*, 275.
(75) Skinner, J. L.; Park, K. *J. Phys. Chem. B* **2001**, *105*, 6716.
(76) Rostkier-Edelstein, D.; Graf, P.; Nitzan, A. *J. Chem. Phys.* **1997**, *107*, 10470.
(77) Rostkier-Edelstein, D.; Graf, P.; Nitzan, A. *J. Chem. Phys.* **1998**, *108*, 9598.
(78) Everitt, K. F.; Skinner, J. L.; Ladanyi, B. M. *J. Chem. Phys.* **2002**, *116*, 179.
(79) Berens, P. H.; White, S. R.; Wilson, K. R. *J. Chem. Phys.* **1981**, *75*, 515.
(80) Frommhold, L. Collision-induced absorption in gases. In *Cambridge Monographs on Atomic, Molecular, and Chemical Physics*, 1st ed.; Cambridge University Press: Cambridge, England, 1993; Vol. 2.
(81) Skinner, J. L. *J. Chem. Phys.* **1997**, *107*, 8717.
(82) An, S. C.; Montrose, C. J.; Litovitz, T. A. *J. Chem. Phys.* **1976**, *64*, 3717.
(83) Egorov, S. A.; Skinner, J. L. *Chem. Phys. Lett.* **1998**, *293*, 439.
(84) Schofield, P. *Phys. Rev. Lett.* **1960**, *4*, 239.
(85) Egelstaff, P. A. *Adv. Phys.* **1962**, *11*, 203.
(86) Kneller, G. R. *Mol. Phys.* **1994**, *83*, 63.
(87) Billing, G. D. *Chem. Phys. Lett.* **1975**, *30*, 391.
(88) Billing, G. D. *J. Chem. Phys.* **1993**, *99*, 5849.
(89) Tully, J. C.; Preston, R. K. *J. Chem. Phys.* **1971**, *55*, 562.
(90) Tully, J. C. *J. Chem. Phys.* **1990**, *93*, 1061.
(91) Kuntz, P. J. *J. Chem. Phys.* **1991**, *95*, 141.
(92) Krylov, A. I.; Gerber, R. B.; Gaveau, M. A.; Mestdagh, J. M.; Schilling, B. *J. Chem. Phys.* **1996**, *104*, 3651.
(93) Yamashita, K.; Miller, W. H. *J. Chem. Phys.* **1985**, *82*, 5475.
(94) Gallicchio, E.; Berne, B. J. *J. Chem. Phys.* **1996**, *105*, 7064.
(95) Gallicchio, E.; Egorov, S. A.; Berne, B. J. *J. Chem. Phys.* **1998**, *109*, 7745.
(96) Egorov, S. A.; Gallicchio, E.; Berne, B. J. *J. Chem. Phys.* **1997**, *107*, 9312.
(97) Krilov, G.; Berne, B. J. *J. Chem. Phys.* **1999**, *111*, 9147.
(98) Rabani, E.; Krilov, G.; Berne, B. J. *J. Chem. Phys.* **2000**, *112*, 2605.
(99) Sim, E.; Krilov, G.; Berne, B. *J. Phys. Chem. A* **2001**, *105*, 2824.
(100) Cao, J.; Voth, G. A. *J. Chem. Phys.* **1994**, *100*, 5093.
(101) Cao, J.; Voth, G. A. *J. Chem. Phys.* **1994**, *100*, 5106.
(102) Cao, J.; Voth, G. A. *J. Chem. Phys.* **1994**, *101*, 6157.
(103) Cao, J.; Voth, G. A. *J. Chem. Phys.* **1994**, *101*, 6168.
(104) Cao, J.; Voth, G. A. *J. Chem. Phys.* **1994**, *101*, 6184.
(105) Voth, G. A. *Adv. Chem. Phys.* **1996**, *93*, 135.
(106) Jang, S.; Voth, G. A. *J. Chem. Phys.* **1999**, *111*, 2357.
(107) Jang, S.; Voth, G. A. *J. Chem. Phys.* **1999**, *111*, 2371.
(108) Reichman, D. R.; Roy, P.-N.; Jang, S.; Voth, G. A. *J. Chem. Phys.* **2000**, *113*, 919.
(109) Calhoun, A.; Pavese, M.; Voth, G. A. *Chem. Phys. Lett.* **1996**, *262*, 415.
(110) Schmitt, U. W.; Voth, G. A. *J. Chem. Phys.* **1999**, *111*, 9361.
(111) Pavese, M.; Voth, G. A. *Chem. Phys. Lett.* **1996**, *249*, 231.
(112) Kinugawa, K.; Moore, P. B.; Klein, M. L. *J. Chem. Phys.* **1997**, *106*, 1154.
(113) Kinugawa, K.; Moore, P. B.; Klein, M. L. *J. Chem. Phys.* **1998**, *109*, 610.
(114) Kinugawa, K. *Chem. Phys. Lett.* **1998**, *292*, 454.
(115) Pavese, M.; Bernard, D. R.; Voth, G. A. *Chem. Phys. Lett.* **1999**, *300*, 93.
(116) Ramirez, R.; Lopez-Ciudad, T.; Noya, J. C. *Phys. Rev. Lett.* **1998**, *81*, 3303.
(117) Ramirez, R.; Lopez-Ciudad, T. *Phys. Rev. Lett.* **1999**, *83*, 4456.
(118) Ramirez, R.; Lopez-Ciudad, T. *J. Chem. Phys.* **1999**, *111*, 3339.
(119) Lopez-Ciudad, T.; Ramirez, R. *J. Chem. Phys.* **2000**, *113*, 10849.
(120) Poulsen, J.; Keiding, S. R.; Rossky, P. J. *Chem. Phys. Lett.* **2001**, *336*, 488.
(121) Poulsen, J.; Rossky, P. J. *J. Chem. Phys.* **2001**, *115*, 8024.
(122) Geva, E.; Shi, Q.; Voth, G. A. *J. Chem. Phys.* **2001**, *115*, 9209.
(123) Shi, Q.; Geva, E. *J. Chem. Phys.* **2002**, *116*, 3223.
(124) Rabani, E.; Reichman, D. R. *J. Chem. Phys.* **2002**, *116*, 6271.
(125) Rabani, E.; Reichman, D. R. *Phys. Rev. E* **2002**, *65*, 036111.
(126) Reichman, D. R.; Rabani, E. *J. Chem. Phys.* **2002**, *116*, 6279.
(127) Wang, H.; Sun, X.; Miller, W. H. *J. Chem. Phys.* **1998**, *108*, 9726.
(128) Pollak, E.; Liao, J. *J. Chem. Phys.* **1998**, *108*, 2733.
(129) Miller, W. H. *Adv. Chem. Phys.* **1974**, *25*, 69.
(130) Miller, W. H. *J. Chem. Phys.* **1970**, *53*, 3578.
(131) Herman, M. F.; Kluk, E. *Chem. Phys.* **1984**, *91*, 27.
(132) Heller, E. J. *J. Chem. Phys.* **1981**, *94*, 2723.
(133) Kay, K. G. *J. Chem. Phys.* **1994**, *100*, 4377.
(134) Ovchinnikov, M.; Apkarian, V. A. *J. Chem. Phys.* **1996**, *105*, 10312.
(135) Ovchinnikov, M.; Apkarian, V. A. *J. Chem. Phys.* **1998**, *108*, 2277.
(136) Sun, X.; Miller, W. H. *J. Chem. Phys.* **1997**, *106*, 916.
(137) Makri, N.; Thompson, K. *Chem. Phys. Lett.* **1998**, *291*, 101.
(138) Miller, W. H. *Faraday, Discuss.* **1998**, *110*, 1.
(139) Shao, J. S.; Makri, N. *J. Phys. Chem. A* **1999**, *103*, 7753.
(140) Thompson, K.; Makri, N. *Phys. Rev. E* **1999**, *59*, R4729.
(141) Kühn, O.; Makri, N. *J. Phys. Chem. A* **1999**, *103*, 9487.
(142) Wang, H.; Thoss, M.; Miller, W. H. *J. Chem. Phys.* **2000**, *112*, 47.
(143) Ovchinnikov, M.; Apkarian, V. A.; Voth, G. A. *J. Chem. Phys.* **2001**, *184*, 7130.
(144) Miller, W. H. *J. Phys. Chem. A* **2001**, *105*, 2942.
(145) Makri, N.; Miller, W. H. *J. Chem. Phys.* **2002**, *116*, 9207.
(146) Sun, X.; Wang, H.; Miller, W. H. *J. Chem. Phys.* **1998**, *109*, 4190.
(147) Sun, X.; Wang, H.; Miller, W. H. *J. Chem. Phys.* **1998**, *109*, 7064.
(148) Wang, H.; Song, X.; Chandler, D.; Miller, W. H. *J. Chem. Phys.* **1999**, *110*, 4828.
(149) Sun, X.; Miller, W. H. *J. Chem. Phys.* **1999**, *110*, 6635.
(150) Vleck, J. H. V. *Proc. Nat. Acad. Sci.* **1928**, *14*, 178.
(151) Gutzwiller, M. C. *J. Math. Phys.* **1967**, *8*, 1979.
(152) Gutzwiller, M. C. *J. Math. Phys.* **1971**, *12*, 343.
(153) Gutzwiller, M. C. *Chaos in Classical and Quantum Mechanics*; Springer-Verlag: Berlin, 1990.
(154) Littlejohn, R. G. *J. Stat. Phys.* **1992**, *68*, 7.
(155) Pechukas, P. *Phys. Rev.* **1969**, *181*, 174.
(156) Levit, S.; Smilansky, U. *Ann. Phys. (N.Y.)* **1977**, *108*, 165.
(157) Levit, S.; Mohring, K.; Smilansky, U.; Dreyfus, T. *Ann. Phys. (N.Y.)* **1978**, *114*, 223.
(158) Maslov, V. P.; Fedoriouk, M. V. *Semiclassical approximation in quantum mechanics*; Reidel: Boston, MA, 1981.
(159) Miller, W. H. *J. Chem. Phys.* **1991**, *95*, 9428.
(160) Heller, E. J. *J. Chem. Phys.* **1991**, *95*, 9431.
(161) Kluk, E.; Herman, M. F.; Davis, H. L. *J. Chem. Phys.* **1986**, *84*, 326.
(162) Kay, K. G. *J. Chem. Phys.* **1994**, *101*, 2250.
(163) Provost, D.; Brumer, P. *Phys. Rev. Lett.* **1995**, *74*, 250.
(164) Garashchuk, S.; Tannor, D. *Chem. Phys. Lett.* **1996**, *262*, 477.
(165) Keshavamurthy, S.; Miller, W. H. *Chem. Phys. Lett.* **1994**, *218*, 183.
(166) Spath, B. W.; Miller, W. H. *J. Chem. Phys.* **1996**, *104*, 95.
(167) Hillery, M.; O'Connell, R. F.; Scully, M. O.; Wigner, E. P. *Phys. Rep.* **1984**, *106* (3), 121.
(168) Imre, K.; Ozizmir, E.; Rosenbaum, M.; Zweifel, P. F. *J. Math. Phys.* **1967**, *8*, 1097.
(169) Shi, Q.; Geva, E. *J. Chem. Phys.* **2003**, *118*, 8173.
(170) Oppenheim, I.; Ross, J. *Phys. Rev.* **1957**, *107*, 28.
(171) Mori, H.; Oppenheim, I.; Ross, J. In *Studies in statistical Mechanics*; De Boer, J., Uhlenbeck, G. E., Eds.; North-Holland: Amsterdam, 1962; Vol. 1.
(172) Hynes, J. T.; Deutch, J. M.; Wang, C. H.; Oppenheim, I. *J. Chem. Phys.* **1968**, *48*, 3085.
(173) Heller, E. J. *J. Chem. Phys.* **1976**, *75*, 1289.
(174) Filinov, V. S.; Bonella, S.; Lazovik, Y. E.; Filinov, A. V.; Zacharov, I. In: *Classical and Quantum Dynamics in Condensed Phase Simulations*; Berne, B. J., Ciccotti, G., Coker, D. F. Ed.; World Scientific: Singapore, 1997.
(175) Berne, B. J.; Thirumalai, D. *Annu. Rev. Phys. Chem.* **1986**, *37*, 401.
(176) Ceperley, D. M. *Rev. Mod. Phys.* **1995**, *67*, 279.
(177) Press, W. H.; Flannery, B. P.; Teukolsky, S. A.; Vetterling, W. T. *Numerical Recipes*; Cambridge University Press: Cambridge, England, 1986.
(178) Chesnoy, J.; Weis, J. J. *J. Chem. Phys.* **1986**, *84*, 5378.
(179) Hautman, J.; Klein, M. L. *Mol. Phys.* **1993**, *80*, 647.
(180) Barker, J. A.; Henderson, D.; Abraham, F. F. *Physica* **1981**, *106A*, 226.
(181) Liao, J. L.; Pollak, E. *J. Chem. Phys.* **2002**, *116*, 2718.